ADP-based for Robust Decentralized Load Frequency Control Schemes to Multi-area Asynchronous Markov Jumping Power Systems with Experience Replay

Hai Wang, Jun Cheng, Shengda Tang, Iyad Katib, Xuan Qiu

I. Case Study 1

In this section, we give a special case to simulate and verify the effectiveness of the algorithm to solve zero-sum games for LFC with Markov jumping parameter. We do not consider the area interconnection case and only consider the LFC control problem for a single-area Markov jumping power system.

The power system under consideration is assumed to have two operating ranges denoted by $\mathcal{M} = \{1, 2\}$ representing "Nominal load" and "Heavy load", respectively. The power system is supposed to jump stochastically between the two modes, and the system parameter values for each mode are shown in the Table I. The corresponding transition rate matrix of the two system modes is given as

$$\Pi = \begin{bmatrix} -3.6 & 3.6 \\ 1.0 & -1.0 \end{bmatrix}.$$

Moreover, the weight matrices are defined as $Q_1 = Q_2 = diag[1, 0.1, 0.1, 1]$, $R_1 = R_2 = 0.01$. Choose the initial controller gain $K_m^{(0)}$ and the external disturbance gain $L_m^{(0)}$ arbitrarily, without loss of generality, and we choose $K_1^{(0)} = K_2^{(0)} = 0$, $L_1^{(0)} = L_2^{(0)} = 0$. While the corresponding eigenvalue of $(\mathbf{A}_m - B_m K_m^{(0)} + F_m L_m^{(0)})$ are listed in Table II, from which we can see that the system will become unstable since the system is not Hurwitz.

Nominal load ($m = 1$)		Heavy load ($m = 2$)	
Parameter	Value	Parameter	Value
T_{g1}	0.073	T_{g2}	0.144
T_{t1}	0.273	T_{t2}	0.535
T_{p1}	15.037	T_{p2}	18.75
K_{p1}	120.3	K_{p2}	150.4
$\tilde{R}_1$	2.0	$\tilde{R}_2$	1.5
K_{e1}	0.6	K_{e2}	0.8

TABLE I: Value of system parameter under different operating conditions

m	Initial $(K_m^{(0)}, L_m^{(0)})$	$\sigma(\mathbf{A}_m^{(0)} - B_m K_m^{(0)} + F_m L_m^{(0)})$
1	$K_1^{(0)} = [0, 0, 0, 0]$ $L_1^{(0)} = [0, 0, 0, 0]$	$\begin{bmatrix} -16.2586 + 0.0000i \\ 1.5529 + 0.0000i \\ -4.9612 + 3.1476i \\ -4.9612 - 3.1476i \end{bmatrix}$
2	$K_2^{(0)} = [0, 0, 0, 0]$ $L_2^{(0)} = [0, 0, 0, 0]$	$\begin{bmatrix} -5.4464 + 1.2859i \\ -5.4464 - 1.2859i \\ -0.2974 + 0.0000i \\ 0.3233 + 0.0000i \end{bmatrix}$

TABLE II: Initial gain pairs and corresponding eigenvalues

Now, let $r_0 = 1$, $x(0) = [0.1, -0.1, 0.1, -0.1]^T$. We simulate the model from $t = 0$ to $t = 10$ sec. All the parameters of the power system, except for the transition rate matrix, are assumed to be unknown. We inject the noises given as

$$e_1 = \sum_{k=1}^{100} \left(0.1 e^{-0.01t} \sin(\omega_k t) + 0.5 \cos(\omega_k t)\right),$$

$$e_2 = e^{-0.01t} + \sum_{k=1}^{100} \sin(\omega_k t),$$

where ω_k, $k = 1, 2, \ldots, 100$, are random numbers uniformly distributed on $[-50, 50]$.

Using the proposed Algorithm 1, we obtain the stabilizing gain pair $(K_m^{(\kappa)}, L_m^{(\kappa)})$ as follows:

$$K_1^{(\kappa)} = [14.3241\ 14.2643\ 4.0943\ 12.3167],$$
$$K_2^{(\kappa)} = [19.5322\ 25.6232\ 4.0504\ 23.1600],$$
$$L_1^{(\kappa)} = [-0.1827\ \ -0.1213\ \ -0.0068\ \ -0.1856],$$
$$L_2^{(\kappa)} = [-0.3172\ \ -0.2978\ \ -0.0184\ \ -0.4462],$$

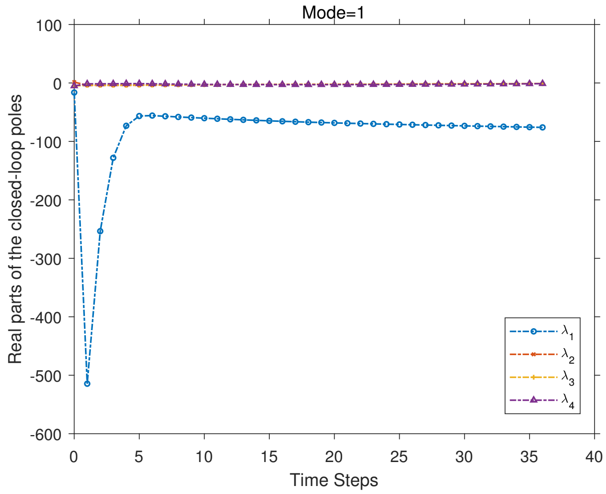

Fig. 1: Real parts of the closed-loop poles via Algorithm 1 in mode 1.

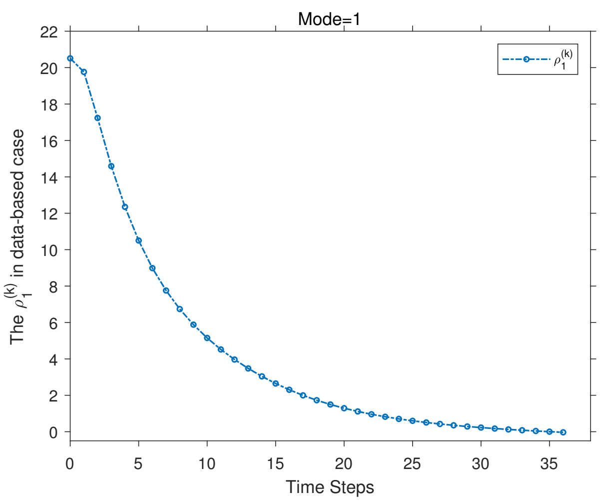

Fig. 2: Trend of $\rho_1^{(k)}$ via Algorithm 1 in mode 1.

and the corresponding eigenvalue is

$$\sigma(\mathbf{A}_1^{(\kappa)} - B_1 K_1^{(\kappa)} + F_1 L_1^{(\kappa)}) = \begin{bmatrix} -75.9512 + 0.0000i \\ -1.0840 + 4.3238i \\ -1.0840 - 4.3238i \\ -1.1335 + 0.0000i \end{bmatrix},$$

$$\sigma(\mathbf{A}_2^{(\kappa)} - B_2 K_2^{(\kappa)} + F_2 L_2^{(\kappa)}) = \begin{bmatrix} -32.9413 + 0.0000i \\ -1.2773 + 4.9580i \\ -1.2773 - 4.9580i \\ -0.9617 + 0.0000i \end{bmatrix},$$

which implies that the gain pair $(K_m^{(\kappa)}, L_m^{(\kappa)})$ is Hurwtiz.

In this simulation scenario, the number of iteration is 36 and 139 respectively, and the process of changing the real part of the eigenvalues is illustrated in Fig. 1-2. In addition, in the case of unknown dynamics, the parameters β_1, β_2 are both set to 20 and the end of the process of finding a stabilizing initial value is marked before the parameter $\rho_m^{(k)}$ becoming negative, see Fig. 3-4 for details of the change in the real part.

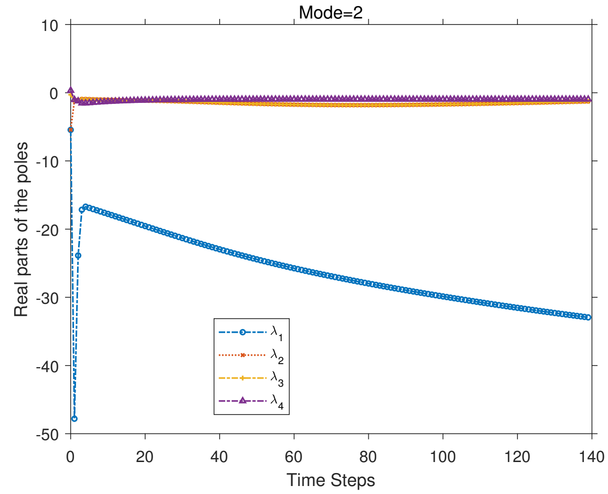

Fig. 3: Real parts of the closed-loop poles via Algorithm 1 in mode 2.

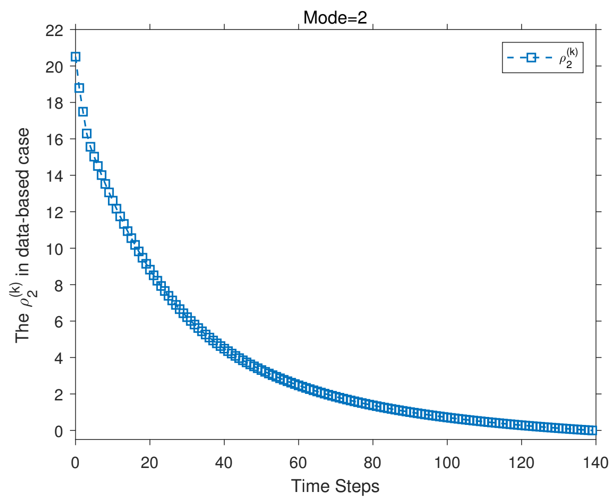

Fig. 4: Trend of $\rho_2^{(k)}$ via Algorithm 1 in mode 2.

For comparison, the optimal $P_m^{(k)}$ obtained by Algorithm 1 and the corresponding matrices P_m^* and K_m^* obtained by [1] are listed in Table III, and we share the norm of the error between $P_m^{(k)}$ and P_m^* as follows:

$$\left\| P_1^{(15)} - P_1^* \right\| = 3.7622 \times 10^{-8},$$
$$\left\| P_2^{(15)} - P_2^* \right\| = 8.5152 \times 10^{-9}.$$

It is obvious that these two groups of results are consistent. The corresponding optimal policy pair $(K_m^{(k)}, L_m^{(k)})$ is shown as follows:

$$\begin{aligned} K_1^{(15)} &= [14.5251 \quad 16.0178 \quad 3.5401 \quad 10.7983], \\ K_2^{(15)} &= [15.0458 \quad 20.6550 \quad 3.7000 \quad 11.4308], \\ L_1^{(15)} &= [-0.1555 \quad -0.1042 \; -0.0069 \quad -0.1330], \\ L_2^{(15)} &= [-0.2382 \quad -0.2237 \; -0.0141 \quad -0.2178]. \end{aligned}$$

Moreover, the convergence of $P_m^{(k)}$ and $K_m^{(k)}$ is illustrated in Fig.5-8 for each corresponding mode. Fig.9-10 depict the

m	Obtained by [1]	Obtained by Algorithm 1
1	$P_1^* = \begin{bmatrix} 0.23818523 & 0.15962699 & 0.01060335 & 0.20360638 \\ 0.15962699 & 0.16691434 & 0.01169301 & 0.13199525 \\ 0.01060335 & 0.01169301 & 0.00258429 & 0.00788275 \\ 0.20360638 & 0.13199525 & 0.00788275 & 1.58693045 \end{bmatrix}$	$P_1^{(15)} = \begin{bmatrix} 0.23818523 & 0.15962699 & 0.01060335 & 0.20360637 \\ 0.15962699 & 0.16691434 & 0.01169301 & 0.13199525 \\ 0.01060335 & 0.01169301 & 0.00258429 & 0.00788275 \\ 0.20360637 & 0.13199525 & 0.00788275 & 1.58693045 \end{bmatrix}$
2	$P_2^* = \begin{bmatrix} 0.36471273 & 0.34253493 & 0.02166601 & 0.33353455 \\ 0.34253493 & 0.44504765 & 0.02974324 & 0.29161237 \\ 0.02166601 & 0.02974324 & 0.00532798 & 0.01646038 \\ 0.33353455 & 0.29161237 & 0.01646038 & 1.63287855 \end{bmatrix}$	$P_2^{(15)} = \begin{bmatrix} 0.36471273 & 0.34253493 & 0.02166601 & 0.33353454 \\ 0.34253493 & 0.44504765 & 0.02974324 & 0.29161237 \\ 0.02166601 & 0.02974324 & 0.00532798 & 0.01646037 \\ 0.33353454 & 0.29161237 & 0.01646037 & 1.63287854 \end{bmatrix}$

TABLE III: Comparison between the results obtained by [1] and the those obtained by Algorithm 1

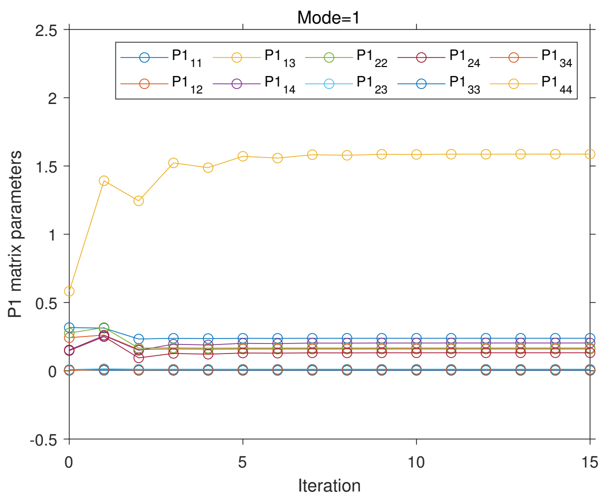

Fig. 5: Convergence of P_1.

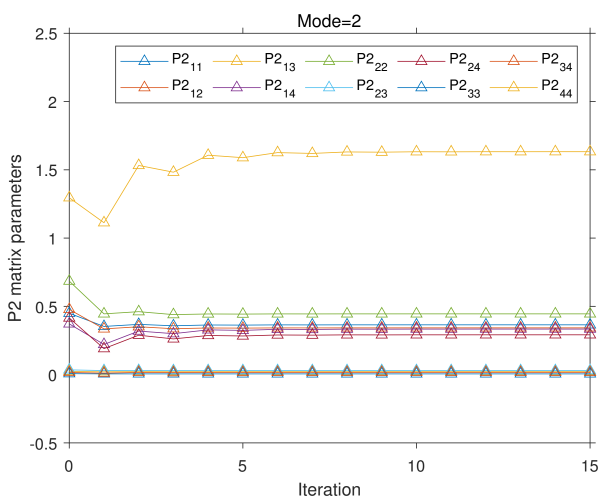

Fig. 6: Convergence of P_2.

control input and external disturbance input respectively, and we can see that the power system eventually becomes stable by applying the initial gain pair $(K_m^{(\kappa)}, L_m^{(\kappa)})$ based on the proposed Algorithm 1.

Now, we apply the optimal control policy and the optimal

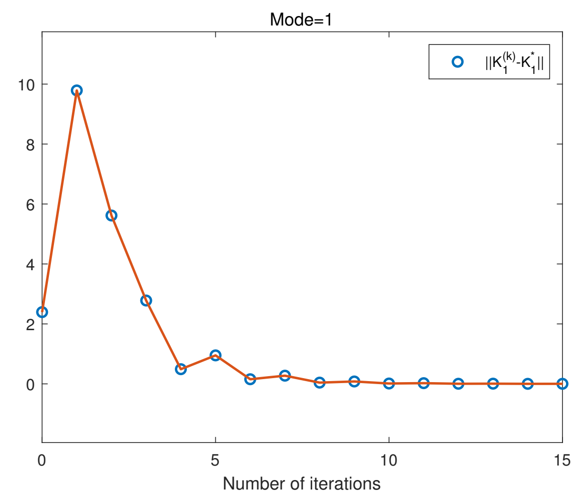

Fig. 7: Optimal K_1 in mode 1.

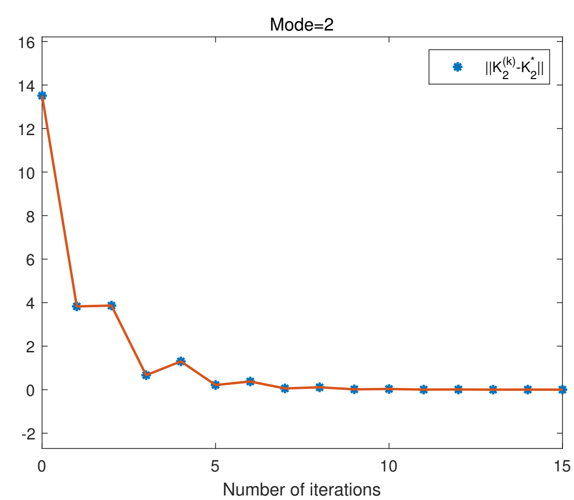

Fig. 8: Optimal K_2 in mode 2.

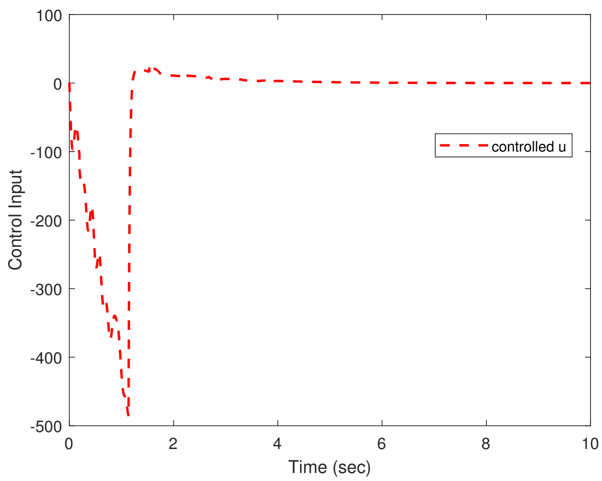

Fig. 9: Control input $u(t)$.

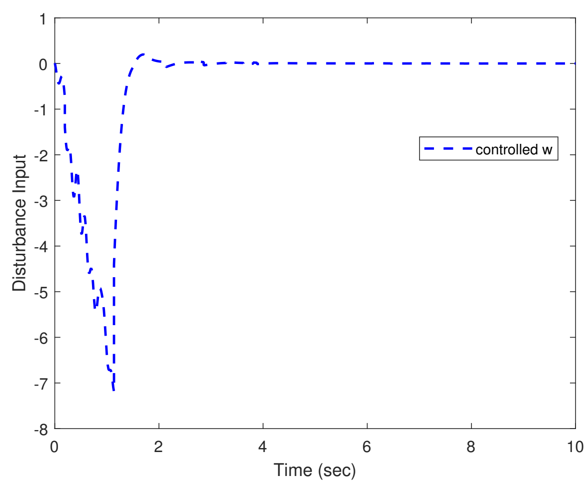

Fig. 10: Disturbance input $w(t)$.

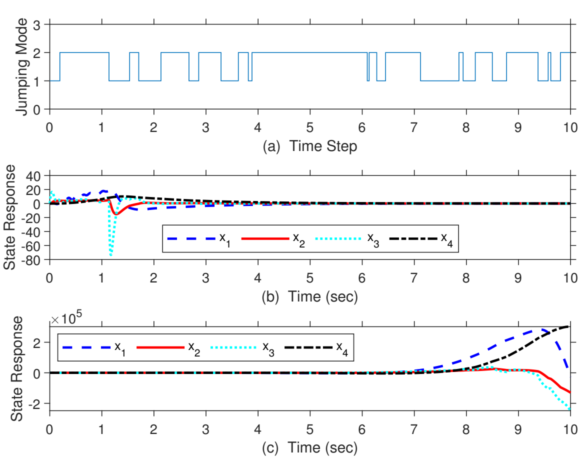

Fig. 11: Jumping mode m and system state response of $x(t)$.

disturbance policy obtained by Algorithm 1 to control the power system to illustrate the effectiveness of the controller designed by the proposed algorithm.

To do that, we consider two application cases. In particularly, during the first two time intervals that the mode switching occurs, a given policy pair is added to the system in both of the two cases, however, from the moment when the third mode switching occurs to the end of the simulation, the policy pair obtained by Algorithm 1 is applied for one case, while the original policy pair is still implemented in the second case. The trajectories of the system in the two cases are plotted in Fig.11. Specially, Fig. 11(a) gives the mode evolution of the power system, Fig. 11(c) describes the state trajectories of the system under the original selected control policy and disturbance policy, and the system is unstable. However, Fig. 11(b) depicts the state trajectories of the system under the optimal policy pair obtained by the Algorithm 1, which implies that the proposed control algorithm is feasible and effective to control the system.

References

[1] H.-N. Wu and B. Luo, “Simultaneous policy update algorithms for learning the solution of linear continuous-time $\mathcal{H}_\infty$ state feedback control ”, *Inf. Sci.* vol. 222, pp. 472-485, Feb. 2013.